Published as: *Neuron*. 2009 May 14; 62(3): 363–374.

Subcellular dynamics of type II PKA in neurons

Haining Zhong[1,2,*], **Gek-Ming Sia**[3,*], **Takashi R. Sato**[1,2], **Noah W. Gray**[1,2], **Tianyi Mao**[1,2], **Zaza Khuchua**[4], **Richard L. Huganir**[3], and **Karel Svoboda**[1,2]

1 *Howard Hughes Medical Institute Janelia Farm Research Campus, Ashburn, VA, 20147*

2 *Cold Spring Harbor Laboratory, Cold Spring Harbor, NY 11724*

3 *Department of Neuroscience, Johns Hopkins University School of Medicine, Baltimore, MD 21205*

4 *Cincinnati Children's Hospital Medical Center, Cincinnati, OH 45229*

SUMMARY

Protein kinase A (PKA) plays multiple roles in neurons. The localization and specificity of PKA are largely controlled by A-kinase anchoring proteins (AKAPs). However, the dynamics of PKA in neurons, and the roles of specific AKAPs, are poorly understood. We imaged the distribution of type II PKA in hippocampal and cortical layer 2/3 pyramidal neurons *in vitro* and *in vivo*. PKA was concentrated in dendritic shafts compared to the soma, axons and dendritic spines. This spatial distribution was imposed by the microtubule-binding protein MAP2, indicating that MAP2 is the dominant AKAP in neurons. Following cAMP elevation, catalytic subunits dissociated from the MAP2-tethered regulatory subunits and rapidly moved to become enriched in nearby spines. The spatial gradient of type II PKA between dendritic shafts and spines was critical for the regulation of synaptic strength and long-term potentiation. The localization and activity-dependent translocation of type II PKA are therefore important determinants of PKA function.

INTRODUCTION

Signaling events mediated by protein kinase A (PKA) are critical for many neuronal functions. PKA is important for learning and memory in *Aplysia*, flies and mice (Abel et al., 1997; Byrne and Kandel, 1996; Dubnau et al., 2003). Consistently, PKA is involved in multiple forms of synaptic plasticity (Blitzer et al., 1998; Brandon et al., 1997; Chevaleyre et al., 2007; Frey et al., 1993; Greenberg et al., 1987; Lu et al., 2007; Tzounopoulos et al., 1998; Weisskopf et al., 1994; Yasuda et al., 2003), including hippocampal long-term potentiation (LTP). PKA has also been implicated in protein trafficking, protein degradation, gene transcription, the regulation of neuronal excitability and other neuronal functions (Choi et al., 2002; Ehlers, 2000; Goldsmith and Abrams, 1992; Greenberg et al., 1987; Hoshi et al., 2005; Impey and Goodman, 2001; Inan et al., 2006; Pedarzani and Storm, 1993).

Protein kinase A (PKA) is a tetrameric protein consisting of two identical regulatory subunits and two catalytic subunits (Francis and Corbin, 1994; Scott, 1991). Each regulatory subunit binds and inhibits a catalytic subunit at the resting state. Binding of cAMP to the regulatory

Address for correspondence: Haining Zhong, Ph.D., Howard Hughes Medical Institute, Janelia Farm Research Campus, 19700 Helix Drive, Room 2C.290, Ashburn, Virginia 20147, USA, Tel: 631-946-0520, E-Mail: E-mail: zhongh@janelia.hhmi.org.
*These authors contribute equally to this work.

subunit releases and activates the catalytic subunit (Figure 1A). PKA isoforms are classified into types I and II based on the regulatory subunits (Francis and Corbin, 1994), with type II, especially IIβ, thought to be the dominant isoform in many neurons (Brandon et al., 1997; Brandon et al., 1998; Ventra et al., 1996).

PKA exerts its function via a wide range of substrates spanning multiple neuronal compartments. For example, at dendritic spines, PKA can phosphorylate AMPA and NMDA glutamate receptors and inhibitor-1, which is an endogenous inhibitor of protein phosphotase-1, to modulate synaptic plasticity (Blitzer et al., 1998; Esteban et al., 2003; Lee et al., 2000; Raman et al., 1996). PKA phosphorylation of AMPA receptors also regulates the sorting of these receptors into recycling or degradation pathways (Ehlers, 2000). In dendrites, PKA phosphorylates stargazin to regulate the trafficking of AMPA receptors (Chetkovich et al., 2002; Choi et al., 2002). PKA also phosphorylates dendritic potassium channels to regulate neuronal excitability (Hoffman and Johnston, 1998; Lin et al., 2008; Pedarzani and Storm, 1993). In addition, PKA plays important roles in transcriptional control (Montminy, 1997; Shaywitz and Greenberg, 1999) and the regulation of the presynaptic terminal (Leenders and Sheng, 2005; Turner et al., 1999; Tzounopoulos et al., 1998; Weisskopf et al., 1994).

Specificity in PKA signaling is believed to arise at least in part from compartmentalization of PKA (Buxton and Brunton, 1983; Rich et al., 2001; Zaccolo and Pozzan, 2002). The subcellular localization of PKA, especially type II PKA, is controlled by A kinase anchoring proteins (AKAPs) (Figure 1A) (Wong and Scott, 2004). AKAPs bind to the N-terminal dimerization domain of PKA regulatory subunits and typically contain a second domain that binds to the cytoskeleton or intracellular scaffolds, thus targeting PKA to specific subcellular locations (Wong and Scott, 2004). More than 50 AKAPs have been identified, many of which are expressed in neurons (Bauman et al., 2004; Tasken and Aandahl, 2004). However, the spatial distribution of PKA in neurons, and how this distribution is shaped by specific AKAPs, is largely unknown. When activated, the catalytic subunit of PKA is released from the regulatory subunit. The spatial range of freed catalytic subunits in neuronal compartments has not been characterized.

We have used two-photon and confocal fluorescence microscopy to measure the distribution of PKA subunits in hippocampal and layer 2/3 pyramidal neurons in dissociated cultures, brain slices and *in vivo*. Type II PKA isoforms were enriched in dendritic shafts compared to dendritic spines. This dendritic targeting was mediated by the microtubule-binding protein MAP2. Catalytic subunits activated by cAMP elevations dissociated from regulatory subunits and rapidly translocated from dendritic shafts to become enriched in spines, presumably to phosphorylate targets in the spine. The spatial regulation of type II PKA is an important determinant of PKA function in neurons.

RESULTS

Type II PKA is enriched in dendrites

To measure the localization of type II PKA in neurons, we tagged the regulatory subunit IIβ (RIIβ) of PKA with monomeric enhanced green fluorescent protein (mEGFP) (Zacharias et al., 2002) at the C-terminus. The cDNAs of RIIβ-mEGFP and a red volume marker (mCherry or DsRed Express) (Shaner et al., 2004) were introduced into cultured hippocampal slices using biolistic gene transfer. Using two-photon laser scanning microscopy, we quantified the relative concentration of RIIβ-mEGFP throughout individual CA1 neurons as the ratio of green fluorescence over red fluorescence (G/R) (Fig 1).

RIIβ-mEGFP was excluded from the nucleus when compared with the red cytosolic marker (Figure 1B4) and enriched in dendrites compared to the soma (Figure 1B3). The concentration

of RIIβ increased with distance from the soma and reached a steady level in apical and basal dendrites (G/R = 227 ± 32% at 57.5μm, normalized to 12.5 μm from the center of soma, n = 6, $p < 0.01$) (Figure 1C, red). A soluble fluorescent protein, monomeric Venus (mVenus), was distributed uniformly throughout the cell (G/R = 97 ± 3%, n = 5, $p > 0.1$) (Figure 1C, black). Higher magnification images in the soma revealed that RIIβ was associated with filamentous structures, likely the microtubule cytoskeleton (Figure 1B5, seen in 6/7 cells). RIIβ was excluded from the axon and presynaptic boutons compared to dendrites (G/R = 28 ± 8%, 50 μm from axon initial segment, 21 ± 5% at distal axon and 16 ± 3% at presynaptic boutons, n = 5, for all values $p < 0.01$) (Figures 1B6, 1B7 and 1D, red). The other type II regulatory subunit, RIIα, was also enriched in dendrites (G/R = 212 ± 22%, n = 6, $p < 0.01$) and excluded from axons (G/R = 27 ± 3% at 50 μm, n = 6, $p < 0.001$) (Figures 1C, 1D, 1E). In contrast, type I regulatory subunits RIα and RIβ were not enriched in dendrites ($G/R_{RI\alpha}$ = 104 ± 7%, n = 6, $p > 0.1$; and $G/R_{RI\beta}$ = 102 ± 5%, n = 5, $p > 0.1$) and only modestly excluded from axons ($G/R_{RI\alpha}$ = 62 ± 4%, n = 9, $p < 0.01$; and $G/R_{RI\beta}$ = 74 ± 6%, n = 7, $p < 0.01$ at 50μm) (Figures 1C, 1D and Supplemental Figure 1). When a mEGFP-tagged catalytic subunit (CAT-mEGFP) was co-expressed with un-tagged RIIβ (Figures 1C, 1D and 1F), the catalytic subunit was also enriched in dendrites compared to soma (G/R = 154 ± 12%, n = 5, $p < 0.02$) and excluded from the axon (G/R = 41 ± 6% at 50μm, n = 6, $p < 0.001$), consistent with the supposition that catalytic subunits bind to regulatory subunits at resting conditions (Francis and Corbin, 1994; Scott, 1991). We conclude that type II PKA is enriched in the dendrite and excluded from the axon in CA1 pyramidal neurons.

Type II PKA is excluded from spines at the resting state

We next analyzed the subcellular distribution of PKA in dendrites and dendritic spines (Figure 2). PKA is thought to reside in spines because PKA has many important postsynaptic functions and several AKAPs are concentrated in the postsynaptic density (Bauman et al., 2004;Gomez et al., 2002;Husi et al., 2000). However, type II PKA subunits were enriched in dendritic shafts compared to neighboring spines (Figures 2A, 2C and 2D), although PKA was still detectable in many spines (Supplemental Figure 2). We computed a spine enrichment index SEI = $\log_2([\text{Green/Red}]_{spine}/[\text{Green/Red}]_{dendrite})$ (Figure 2D). A positive SEI implies enrichment in the spine; whereas a negative value indicates exclusion from the spine. As a control, the soluble protein mVenus had a SEI close to zero (0.043 ± 0.004, n = 42) (Figures 2C6 and 2D). Both RIIα and RIIβ had negative SEI values ($SEI_{RII\alpha}$ = − 1.29 ± 0.07, n = 59, $p < 0.001$; and $SEI_{RII\beta}$ = − 1.28 ± 0.06, n = 83, $p < 0.001$) (Figures 2C and 2D), indicating that they were excluded from spines. In contrast, RIα and RIβ distributed evenly between dendrite and spine ($SEI_{RI\alpha}$ = − 0.097 ± 0.04, n = 74, p = 0.015; and $SEI_{RI\beta}$ = − 0.11 ± 0.05, n = 72, p = 0.025; α = 0.0017 after Bonferroni correction for the 6 tests). When co-expressed with RIIβ, CAT-mEGFP was also excluded from spines (SEI = − 0.84 ± 0.05, n = 63, $p < 0.001$) (Figure 2A, 2C3 and 2D). A similar subcellular distribution of type II PKA was observed in CA3 neurons (Supplemental Figure 3). However, CAT-mEGFP was not excluded from spines under these conditions when expressed alone, possibly because over-expressed catalytic subunits saturated endogenous regulatory subunits (data not shown). Finally, SEIs and spine volumes were not correlated (Supplemental Figure 4).

We next tested if type II PKA was also excluded from dendritic spines in living mice. CAT-mEGFP, RIIβ and DsRed Express were introduced into layer 2/3 pyramidal neurons in the somatosensory cortex using in utero electroporation (Gray et al., 2006; Saito and Nakatsuji, 2001; Tabata and Nakajima, 2001). CAT-mEGFP was excluded from spines in acute brain slices prepared from 2–3 week old mice (SEI = − 0.693 ± 0.04, n = 31, $p < 0.001$) (Figure 2B and 2D). Consistently, CAT-mEGFP was also excluded from spines in living adolescent mice (SEI = − 0.57 ± 0.05, n = 69, $p < 0.001$) (Figure 2B and 2D). We conclude that type II PKA is enriched in dendritic shafts compared to spines in pyramidal neurons.

Endogenous PKA is excluded from spines

Over-expression of PKA or tagging PKA with fluorescent proteins could perturb the spatial distribution of PKA in neurons. We therefore measured directly the distribution of endogenous PKA using immunocytochemistry. Dissociated cultures of rat hippocampal neurons were transfected with the cytosolic marker EGFP and stained using an antibody against the PKA catalytic subunits (PKA-NT, US Biologicals) (Figure 2D and 2E1). The specificity of the antibody was verified by western blots and by immunostainings using the antibody pre-incubated with the antigen peptide (Supplemental Figure 5, see also Supplemental Figure 9A). Endogenous PKA catalytic subunits were enriched in the dendritic shaft compared to neighboring spines (SEI = − 1.8 ± 0.16, n = 35, $p < 0.001$). Similar results were obtained using a second antibody against the PKA catalytic subunits (Supplemental Figure 5C). Furthermore, endogenous PKA RIIβ was also enriched in dendritic shafts compared to spines (SEI = − 1.30 ± 0.12, n = 36, $p < 0.001$) (Figure 2D, 2E2 and Supplemental Figure 5). In addition, CAT-mEGFP was enriched in dendritic shafts in layer 2/3 pyramidal neurons in brain slices even without co-expression of RIIβ (SEI = − 0.598 ± 0.06, n = 41, $p < 0.001$) (Figures 2B3 and 2D). This indicates that endogenous regulatory subunits were also excluded from spines and were probably in excess of endogenous catalytic subunits. Finally, over-expression and tagging with fluorescence proteins are more likely to disrupt, rather than create, the PKA gradient we observed. Indeed, computer simulations indicate that increasing RIIβ concentration by over-expression is likely to have minimal effects on SEI values (Supplemental Figure 6). When RIIβ concentrations approach AKAP concentrations, the PKA gradient collapses. These results show that in the resting state endogenous PKA is enriched in dendritic shafts compared to dendritic spines.

Dendritic targeting of PKA is mediated by MAP2

To identify the mechanisms of type II PKA localization, we carried out a deletion analysis of the regulatory subunit. The N-terminal 47 residues of RIIβ, which contain the dimerization domain and the AKAP-binding domain, were sufficient for the spine exclusion (SEI = − 2.04 ± 0.08, n = 42, $p < 0.001$) (Figure 3A). A previous study showed that deleting the first five residues (S2-I6) of RIIα disrupted its binding to AKAPs without affecting dimerization and other functions (Hausken et al., 1994). Deleting these residues in RIIα and the corresponding sequences in RIIβ results in mutants (RIIα-Δ 2–6 and RIIβ-Δ 2–5 respectively) that expressed at a level similar to that of the wild-type subunits in neurons (Supplemental Figure 7). However, the PKA gradient from dendritic shafts to spines was disrupted ($SEI_{RIIα\text{-}Δ\ 2\text{-}6}$ = − 0.19 ± 0.04, n = 76, $p < 0.001$ c.f. RIIα; and $SEI_{RIIβ\text{-}Δ\ 2\text{-}5}$ = 0.15 ± 0.05, n = 60, $p < 0.001$ c.f. RIIβ) (Figure 3A). Thus, a dendritically-localized AKAP is responsible for concentrating type II PKA in dendritic shafts.

The distribution of type II PKA resembled that of the abundant microtubule-binding protein MAP2 (Dehmelt and Halpain, 2005), which was the first AKAP identified (Theurkauf and Vallee, 1982). Indeed, linking the microtubule binding domain (MTBD) of MAP2 to RIIβ-Δ 2–5, which by itself does not bind AKAPs and distributes evenly between the dendritic shaft and spines, restored the spine exclusion (SEI = − 1.86 ± 0.1, n = 40, $p < 0.001$ c.f. RIIβ-Δ 2–5) (Figure 3A). To test if MAP2 is necessary for dendritic localization of PKA, we analyzed the subcellular distribution of RIIβ-mEGFP in CA1 neurons in cultured hippocampal slices prepared from mice in which the PKA binding site of MAP2 was genetically deleted (*MAP2Δ1–158*) (Khuchua et al., 2003). The localization of RIIβ-mEGFP was partially disrupted in heterozygous neurons (SEI_{wt} = −1.61 ± 0.07; and $SEI_{heterozygous}$ = − 0.97 ± 0.07, n = 84; $p < 0.001$) (Figures 3B and 3C). In homozygous neurons RIIβ-mEGFP even became slightly enriched in spines (SEI = 0.50 ± 0.04, n = 83, $p < 0.001$), possibly by binding to other AKAPs in spines that are dominated by MAP2 in wild-type neurons (Figures 3B and 3C). Under our experimental conditions spines occupy ~ 6 % of the dendritic volume (see Methods).

An SEI value of −1.61 in wild-type neurons implies that nearly 98% of total RIIβ is restricted to dendritic shafts by MAP2. We conclude that, whereas other AKAPs are present in neurons, MAP2 is the dominant AKAP in pyramidal neurons that anchors type II PKA to dendritic shafts.

Activated PKA catalytic subunit translocates to become enriched in spines

We next asked whether the distribution of PKA changes upon activation by cAMP. Neurons in hippocampal slices expressing CAT-mEGFP, RIIβ and mCherry were stimulated by bath application of 50 μM forskolin, an adenylyl cyclase activator, and 100 μM IBMX, a phosphodiesterase inhibitor, which cause intracellular cAMP elevations. CAT-mEGFP moved rapidly into spines upon stimulation where it remained as long as forskolin and IBMX were present ($SEI_{before} = -0.84 \pm 0.05$; and $SEI_{after} = 0.442 \pm 0.03$; $n = 63$, $p < 0.001$) (Figures 4A, 4B and 4D). Activated CAT-mEGFP even became enriched in spines as indicated by the positive SEI value ($p < 0.001$). The distribution of RIIβ-mEGFP did not change upon activation ($SEI_{before} = -1.66 \pm 0.07$; and $SEI_{after} = -1.81 \pm 0.07$; $n = 33$, $p = 0.14$) (Figure 4C). The catalytic subunit showed similar dynamics in cortical layer 2/3 neurons in acute brain slices from mice electroporated with CAT-mEGFP and DsRed Express, both with and without RIIβ (Figure 4E). Furthermore, endogenous cAMP activators, such as the neuromodulators norepinephrine (NE) (Raman et al., 1996) and dopamine (Otmakhova and Lisman, 1998), were sufficient to trigger translocation of the catalytic subunit into spines ($SEI_{before} = -1.04 \pm 0.09$; and $SEI_{after} = -0.35 \pm 0.10$; $n = 41$, $p < 0.001$) (Figure 4F and data not shown), although these effects were weaker compared to forskolin and IBMX stimulation. These data suggest that catalytic subunits dissociate from type II regulatory subunits in the presence of cAMP. Although the regulatory subunits are still anchored in dendrites, freed catalytic subunits translocate, probably by diffusion, into spines. These freed catalytic subunits become enriched in spines, presumably by binding to abundant PKA targets in spines.

The mobility of PKA catalytic subunits increases with activation

This view of PKA dynamics was further supported by direct measurements of PKA mobility. The catalytic subunit was tagged with a photoactivatable fluorescent protein (mPAGFP) (Patterson and Lippincott-Schwartz, 2002) and co-expressed with RIIβ and mCherry in CA1 neurons. The effective diffusion of the catalytic subunit was measured as the decay time constant of CAT-mPAGFP fluorescence following nearly instantaneous (20 ms) photoactivation in a small region of interest (see Experimental procedures) (Bloodgood and Sabatini, 2005; Gray et al., 2006). CAT-mPAGFP was more mobile in dendritic shafts after the application of forskolin/IBMX compared to resting conditions ($\tau_{before=}12.3 \pm 1.9$ s; and $\tau_{after} = 6.1 \pm 1.5$ s; $n = 15$, $p < 0.001$, sign test) (Figure 5). The diffusional relaxation of photoactivated CAT-mPAGFP was complex, even in elevated cAMP (Figure 5B and data not shown). The decay curves suggest the presence of slowly and rapidly diffusing populations of molecules, perhaps reflecting an incomplete release of the catalytic subunits from the regulatory subunits. In contrast to the diffusion in dendritic shafts, the effective diffusion in spines was similar before and after cAMP elevation ($\tau_{before} = 4.6 \pm 0.6$ s; and $\tau_{after} = 4.5 \pm 0.4$ s; $n = 17$, $p = 1$). These measurements show that cAMP elevations increase the diffusional mobility of PKA catalytic subunits in dendritic shafts.

PKA localization shapes synaptic strength

PKA phosphorylation of AMPA receptors facilitates their insertion into synapses (Esteban et al., 2003; Lee et al., 2000; Man et al., 2007; Oh et al., 2006; Sun et al., 2005; Swayze et al., 2004). We therefore asked whether the spatial gradient of PKA between the dendritic shaft and spines is important for regulating the postsynaptic sensitivity to glutamate. We expressed wild-type RIIβ-mEGFP in layer 2/3 cortical neurons and measured the AMPA receptor-mediated

glutamate sensitivity at individual spines synapses in acute brain slices (P14–P21) using two-photon glutamate uncaging (Carter and Sabatini, 2004; Matsuzaki et al., 2001; Sobczyk et al., 2005). We tuned the parameters so that the resulting uncaging-evoked excitatory postsynaptic currents (uEPSC, − 11.6 ± 1.2 pA) mimic the size of miniature EPSCs in layer 2/3 pyramidal neurons (15 – 20 pA) (Myme et al., 2003). To minimize variability, we also performed control measurements from untransfected cells in the same set of brain slices under matched conditions.

The volumes of the stimulated spines were similar between transfected neurons and untransfected controls in the same slices (normalized volumes $V_{RII\beta}$ = 96 ± 5%, n = 100; vs. $V_{same\text{-}slice\ control}$ = 100 ± 5%, n = 82; p = 0.53). However, transfected neurons had significantly smaller uEPSC than untransfected neurons ($uEPSC_{RII\beta}$ = 67 ± 4%; vs. $uEPSC_{same\text{-}slice\ control}$ =100 ± 10%; p < 0.002) (Figure 6). The RIIβ mutant (RIIβ-Δ 2–5), which cannot bind AKAPs and distributes evenly between dendritic shaft and spines, did not show this dominant-negative effect ($uEPSC_{RII\beta\text{-}\Delta\ 2\text{–}5}$ = 93 ± 6%, n = 97; vs. $uEPSC_{same\text{-}slice\ control}$ = 100 ± 7%, n = 85; p = 0.43; and $V_{RII\beta\text{-}\Delta\ 2\text{–}5}$ = 105 ± 6%; vs. $V_{same\text{-}slice\ control}$ = 100 ± 6%; p = 0.57). However, tethering the microtubule-binding domain of MAP2 to the mutant RIIβ RIIβ-Δ 2–5-MTBD) rescued the dominant-negative effect ($uEPSC_{RII\beta\text{-}\Delta\ 2\text{–}5\text{-}MTBD}$ = 72 ± 5%, n = 85; vs. $uEPSC_{same\text{-}slice\ control}$ = 100 ± 11%, n = 75; p < 0.02; and $V_{RII\beta\text{-}\Delta\ 2\text{–}5\text{-}MTBD}$ = 92 ± 4%; vs. $V_{same\text{-}slice\ control}$ = 100 ± 5%; p = 0.25). Computer simulations suggest that overexpression of wild-type RIIβ, but not AKAP-binding deficient mutant RIIβ, can lead to a large reduction in PKA activity in spines induced by transient cAMP (Supplemental Figure 8). These results imply that overexpression of RIIβ reduces PKA activity in spines, leading to decreased AMPA receptor-mediated glutamate sensitivity. Taken together, the MAP2-mediated PKA localization is important in setting the strength of excitatory synapses.

PKA localization modulates LTP induction

The strength of excitatory synapses is regulated by activity-dependent synaptic plasticity, such as long-term potentiation (LTP). Activation of the PKA-activating β-adrenergic receptors by norepinephrine (NE) enhances the magnitude of LTP induced by relatively weak synaptic stimuli (Gelinas and Nguyen, 2005; Gelinas et al., 2008; Hu et al., 2007; Thomas et al., 1996; Winder et al., 1999). We therefore asked whether the MAP2-mediated anchoring of type II PKA to dendritic shafts regulates LTP induction. We first examined whether standard LTP induced with tetanic stimulation (2 × 100 Hz × 1s, 30s interval) is impaired in CA1 of *MAP2Δ1–158* mice, in which the binding between PKA and MAP2 but not with other AKAPs is disrupted. LTP in brain slices from homozygous mice (−/−) was not significantly different from heterozygous or wild-type littermates (potentiation P_{wt} = 59 ± 6%, n = 10; $P_{heterozygous}$ = 54 ± 7%, n = 7; and $P_{homozygous}$ = 49 ± 9%, n = 10, homozygous) (Figure 7).

We next examined if the binding between MAP2 and PKA is required for the facilitation of LTP in response to weaker stimuli (900 pulses at 10 Hz). Norepinephrine enhanced the potentiation in wild-type mice (P_{NE} = 47 ± 6%, n = 8; and $P_{control}$ = 20 ± 4%, n = 6; p < 0.01). However, this enhancement was absent in heterozygous (P_{NE} = 21 ± 5%, n = 8; p < 0.01 c.f. wild-type ; and $P_{control}$ = 12 ± 6%, n = 9) and homozygous mice (P_{NE} = 19 ± 8%, n = 11; p < 0.02 c.f. wild-type ; and $P_{control}$ = 15 ± 6%, n = 11) (Figure 7). This is consistent with the observation that localization of type II PKA is disturbed even in heterozygous neurons (Figure 3C). The expression levels of the PKA catalytic subunit and RIIβ were not reduced in the hippocampus of the mutant mice (Supplemental Figure 9). Our results therefore suggest that mislocalization of type II PKA might lead to defective phosphorylation of PKA substrates and misregulation of LTP thresholds. Indeed, we found that epinephrine-induced GluR1 phosphorylation was abnormal in *MAP2Δ1–158* mice (Supplemental Figure 10). We conclude that the MAP2 anchoring of type II PKA to dendritic shafts is critical for norepinephrine facilitation of LTP induction. Since *MAP2Δ1–158* mice have deficits in contextual fear

conditioning, our results suggest that modulation of LTP by the stress hormone norepinephrine might be an important synaptic mechanism underlying learned fear.

DISCUSSION

We measured the subcellular distribution of PKA in hippocampal and cortical layer 2/3 pyramidal neurons *in vitro* and *in vivo*. Type II PKA was enriched in dendrites compared to dendritic spines less than one micrometer away. Type II PKA was also excluded from axons and presynaptic terminals. The localization of type II PKA catalytic subunits was regulated by cAMP such that activated catalytic subunits translocated from dendritic shafts to become enriched in spines. This spatial regulation of PKA was important for controlling the glutamate sensitivity of dendritic spines, for regulating glutamate receptor phosphorylation and for PKA-meditated enhancement of LTP induction.

Our results confirm previous studies of the distribution of PKA at the level of large neuronal compartments such as the soma, proximal dendrite and proximal axon (De Camilli et al., 1986). However, the finding that PKA is excluded from dendritic spines is surprising. PKA is generally thought to be enriched in spines via synaptically localized AKAPs such as AKAP79/150 and Yotiao (Bauman et al., 2004; Carr et al., 1992; Lin et al., 1998; Tunquist et al., 2008; Westphal et al., 1999). In contrast, we find that dendritic MAP2 is the dominant AKAP in pyramidal dendrites, restriciting > 97% of total RII subunits to dendritic shafts. These results are consistent with previous observations in MAP2 knock-out mice showing that type II PKA subunits are largely lost in proximal hippocampal dendrites (Harada et al., 2002). On the other hand, our results are at odds with a recent study suggesting that type II PKA is concentrated in dendritic spines in an AKAP150-dependent manner (Tunquist et al., 2008). However, this study does not provide quantification of PKA subunit distributions and suffers from a lack of direct comparison with an evenly-distributed cytosolic marker. RIIβ has a very high affinity for the synaptically localized AKAP79/150 (Herberg et al., 2000). Our results therefore imply that MAP2 is more abundant than all other AKAPs taken together.

Interactions between AKAPs and type II PKA have previously been shown to influence excitatory synaptic transmission (Rosenmund et al., 1994; Snyder et al., 2005), but the underlying mechanism is not clear. Our results indicate that the interaction between MAP2 and type II PKA is an important regulator of postsynaptic function in synapses, possibly by enhancing LTP during behavioral salient conditions. Consistently, *MAP2Δ1–158* mice have a profound deficit in contextual fear conditioning (Khuchua et al., 2003). Furthermore, LTP is impaired even in heterozygous *MAP2Δ1–158* mice (Figure 7), in which PKA has only a slightly higher tendency to go into dendritic spines compared to wide-type mice (Figure 3C). It therefore appears that regulating PKA access to spines is functionally extremely important. Finally, LTP triggered by tetanic stimuli is not impaired in these mice, confirming that PKA likely plays a regulatory rather than an obligatory role in synaptic plasticity (Iyengar, 1996). Our study does not exclude important roles for other AKAPs in the postsynaptic density, such as AKAP79/150 (Bauman et al., 2004; Lu et al., 2007; Lu et al., 2008; Swayze et al., 2004; Tavalin et al., ; Tunquist et al., 2008). Aspects of synaptic plasticity are impaired in mice lacking the PKA binding site of AKAP150 (Lu et al., 2007; Lu et al., 2008). These synaptic AKAPs might recruit a low concentration of PKA into spines to phosphorylate specific targets, even though the major PKA reservoir resides in dendritic shafts. The precise functional differences of synaptic AKAPs and dendritic MAP2 remain to be identified.

PKA phosphorylation of S845 is important for the insertion of GluR1-containing AMPA receptors into synapses (Esteban et al., 2003; Lee et al., 2000; Man et al., 2007; Oh et al., 2006; Sun et al., 2005; Swayze et al., 2004). We found that adrenergically-induced GluR1 phosphorylation is abnormal in *MAP2Δ1–158* mice, suggesting that the AMPA receptor is one

of the substrates of MAP2-anchored PKA. How does PKA in dendritic shafts influence synaptic AMPA receptors and other synaptic substrates? We found that activated PKA catalytic subunits translocate from dendritic shafts to become enriched in dendritic spines. This phenomenon indicates that catalytic subunits bind to immobile partners in spines, which likely correspond to PKA substrates.

Although PKA is commonly thought to be localized close to its substrates via AKAPs, our finding suggests the inverse: AKAPs also play an important role in isolating the majority of PKA from its targets in the postsynaptic density until PKA is activated. Similar dynamics has been observed for calcium/calmodulin kinase II (CaMKII), which can also translocate from dendrites into spines in response to elevations of calcium (Gleason et al., 2003; Meyer and Shen, 2000; Shen and Meyer, 1999). One beneficial consequence of such spatial regulation would be to minimize the effects of basal kinase activity on critical synaptic targets.

In contrast to type II PKA, we have found that type I PKA distributes rather evenly throughout the cell, in agreement with the thinking that type I PKA isoforms are mostly cytosolic (Francis and Corbin, 1994; Scott, 1991). At dendrites, the endogenous PKA distribution mimics that of the type II PKA, suggesting that type II subunits are dominant over the type I subunits, consistent with the predominantly postsynaptic phenotypes in RIIβ knock-out mice (Inan et al., 2006). On the other hand, the observation that type I PKA is relatively enriched in axons and presynaptic terminals compared to type II PKA, is consistent with a dominant role of type I PKA in axons (Brandon et al., 1997).

Finally, we have found that PKA catalytic subunits rapidly move in and out of spines within seconds. PKA activity is therefore not expected to be spine-specific unless PKA is inactivated within several seconds. This is in agreement with the recent finding that synaptic plasticity at individual spines can influence the signaling of neighboring spines (Harvey and Svoboda, 2007). Overall, our results provide a basis for understanding PKA signaling in neurons.

EXPERIMENTAL PROCEDURES

Molecular Biology

cDNA constructs were made with standard subcloning methods. RIIα, RIα, RIβ and the catalytic subunit (type α) were from mouse and RIIβ was from rat. A his-tag at the N-terminus of RIα and RIβ that came from the original cDNA was not removed. mEGFP (EGFP, A206K) (Zacharias et al., 2002) was tethered to the end of the protein with a 2-amino-acid-residue linker DI (EcoRV site) for all regulatory subunits. The end of the catalytic subunit was tethered to mEGFP (without M1 and V1a) with the linker IDYDVPDYASLM. Similar tagging did not interfere with PKA functions (Zaccolo and Pozzan, 2002). DsRed Express was from Clontech and mCherry was derived from mRFP (Shaner et al., 2004). cDNA constructs were subcloned into pCDNA3 or pRK5 for transient expression in cultured hippocampal slices and a custom vector for *in utero* electroporation (Gray et al., 2006).

Transfection

Hippocampal neurons in cultured brain slices were transfected using biolistic gene transfer (Helios, Bio-Rad, 1.6μm gold beads). Layer 2/3 neurons were transfected by in utero electropotation of E16 mouse embryos using a custom electroporator (Gray et al., 2006). Dissociated neuronal cultured were transduced with lentiviral particles containing the GFP transgene.

Organotypic slice culture

Cultured hippocampal slices were prepared (Stoppini et al., 1991) from P6–7 rats or mice in accordance with the animal care and use guidelines of Cold Spring Harbor Laboratory and Janelia Farm Research Institute. Experiments were performed at 8–16 days in vitro.

Acute slice preparation

Coronal brain slices (300 μm thick) were prepared from mice with transfected Layer 2/3 neurons in accordance with institutional animal care and use guidelines. The cutting solution (gassed with 95% O_2/5% CO_2) contained (in mM) 110 choline chloride, 25 $NaHCO_3$, 25 D-glucose, 2.5 KCl, 7 $MgCl_2$, 0.5 $CaCl_2$, 1.25 NaH_2PO_4, 11.5 sodium ascorbate and 3 sodium pyruvate. The slices were incubated in gassed artificial cerebral spinal fluid (ACSF) containing 127 NaCl, 25 $NaHCO_3$, 25 D-glucose, 2.5 KCl, 1 $MgCl_2$, 2 $CaCl_2$, and 1.25 NaH_2PO_4 at 35° C for 30 minutes and then at room temperature for up to 6 hours.

For LTP experiments, 400 μm thick coronal brain slices were sliced and recovered in gassed ACSF containing 1.3 $MgCl_2$, 2.5 $CaCl_2$.

Imaging

For brain slice experiments we used a custom-built two-photon microscope controlled by ScanImage (Pologruto et al., 2003). Two Ti:sapphire lasers (MaiTai, Spectra Physics) were combined with polarized optics and passed through the same set of scan mirrors and objective for simultaneous imaging and photoactivation/uncaging. Unless specified, a water-immersion objective from Olympus (60 ×, 0.9 NA) was used. Experiments were performed at room temperature. Cultured hippocampal slices or acute brain slices were circularly perfused with gassed ACSF containing 4mM Ca^{2+} and 4 mM Mg^{2+}. The imaging laser was tuned to 960 nm to simultaneously excite mEGFP and red fluorescent proteins (mCherry or DsRed Express). For experiments involving DsRed Express, a small amount of bleed-through into the green channel (~3%) was corrected in calculations (e.g. Figure 1B and 2B). Both red proteins gave equivalent results, and all results were pooled together. The images from different color channels were individually adjusted for brightness and contrast before combined into a color image. Stocks of forskolin, IBMX and norepinephrine (CalBiochem) were added to the circulating reservoir of ACSF where applicable. Imaging of layer 2/3 neurons in living mice was as described (Gray et al., 2006).

Photoactivation

For these experiments the wavelength for imaging was 990 nm to excite PAGFP and mCherry while minimizing basal photoactivation. 810 nm was used for photoactivation. Time-lapse images were acquired every 0.256 s. The photoactivating illumination was applied at the 11^{th} frame within a small region of interest at a power empirically determined at the time of experiment. The location, timing and intensity of the photoactivating stimulus were identical before and after the forskolin/IBMX treatment (Figure 5). To average multiple trials, the integrated signal of PAGFP (green channel) within a region of interest was normalized by the red signal at the 1^{st} frame before averaging, to minimize possible movement-related drift between trials. The resulting traces were fit with a single exponential, $F=Ae^{-(t/\tau)} + B$.

Electrophysiology and glutamate uncaging

Whole-cell voltage-clamp recording were performed using an Axopatch 200B amplifier (Axon). Electrophysiological signals were digitized at 10 kHz and acquired with custom software synchronized with ScanImage. The internal solution contained (in mM) 132 K-gluconate, 10 HEPES, 10 Na-phosphocreatine, 4 $MgCl_2$, 4 Na_2-ATP, 0.4 Na-GTP, 3 Na-ascorbate and 0.02 Alexa 594, with osmolarity 295. Cells were held at − 80 mV.

For LTP experiments we used 3–6 weeks old mice. Field potentials were measured at room temperature in stratum radiatum (~100 μm from CA1 cell bodies) using a glass electrode (1–2 MΩ) filled with perfusion solution (ACSF containing 1.3 $MgCl_2$, 2.5 $CaCl_2$). Synaptic responses (0.1–0.5 mV) were evoked with a monopolar glass electrode with single voltage pulse (200 μs, 20–40V), placed 100 μm laterally from the recording electrode along the Schaffer collateral axons. Test stimuli were provided every 30s. 2 train of 100 Hz stimuli with 30s interval or 900 pulses of 10 Hz stimulation were used to trigger LTP as indicated. In some experiments 10 μM NE was applied from 15 to 5 min before LTP induction.

For glutamate uncaging, 2.5 mM MNI-caged-L-glutamate (Tocris) was added to the ACSF, together with 5μM R-CPP and 1μM TTX. To achieve photolysis the laser beam was parked at the tip of the spine head in the direction away from the parent dendrite. Test pulses (1 ms duration) were delivered at 0.1 Hz. The power was 60 mW in the objective back focal plane, of which approximately 18% was transmitted through the objective. Only spines that were well separated from both the dendrite and neighboring spines were selected for analysis. The uncaging depth in the slice was restricted to 10–40 μm. uEPSCs amplitudes were measured, based on averages of 4 trials, as the difference between the mean current amplitude over a 2 ms window around the peak and the mean current amplitude over a 100 ms window before the stimulus.

Data analysis

Measurements were performed using custom software written in Matlab. For spine enrichment index (SEI) measurements, regions of interest (ROIs) were drawn manually on the x–y max projection of a spine and its parent dendrite. The green (G) and red (R) signals within the ROIs were then averaged after background subtraction (from a manually selected background ROI) for three consecutive z slices (1 μm z steps) with the middle z slice giving the highest integrated value in red among all z slices. SEI is defined as $\log_2([G/R]_{spine}/[G/R]_{dendrite})$.

The fraction of PKA in dendritic shafts was calculated based on a recent study using electron microscopy (Zito et al., 2009). Two segments of thin dendrites (diameter being 1.0 and 1.1 μm respectively; and length being 65 and 44 μm respectively) contain 18 and 22 spines respectively. The averaged volume of the spines was measured to be 0.13fL. The relative spine volume compared to the total volume (spine and dendrite) is calculated to be $V_{spine} = 6\%$. The fraction of PKA in dendritic shafts was calculated as $(1-V_{spine})/[2^{SEI} V_{spine} + (1-V_{spine})]$.

For Figure 1C, the soma center was determined as follows: an ROI was drawn around the soma. The soma was segmented by thresholding (background + 3 X SD). The center was the point transected by three orthogonal planes which divide the soma in half. The ratios of average green over average red were calculated from background subtracted pixels that were binned every 5μm along the radius away from the center.

Averaged data are presented as mean ± sem unless noted otherwise. n indicates the number of experiments. p values are from t tests, unless noted otherwise.

Dissociated neuronal culture and immunostaining imaging

Dissociated hippocampal neurons from E18 rat pups were plated onto poly-lysine coated coverslips in Neurobasal-A medium (Invitrogen) supplemented with 2% B27, 1 mM Glutamax, and 5% equine serum (Hyclone). 50 μM FDUR was added after 5 days. Every 3–4 days, half of the medium was removed and replaced with fresh plating medium with equine serum omitted. At DIV 14, cultures were transduced with lentiviral particles containing the GFP transgene.

At DIV 28, cultures were fixed in 4% paraformaldehyde, 4% sucrose in PBS for 30 min at room temperature, then permeabilized with 0.2% Triton X-100 in PBS on ice for 10 min. The coverslips were then blocked with 10% normal goat serum in PBS for 1 hr followed by incubation with primary antibodies (mouse anti-GFP, 1:1000, Chemicon MAB3580, rabbit anti GFP, home-made, rabbit anti-PKA catalytic subunit (PKA-NT), 10 μg/ml, USA Biologicals #P9102-91A, mouse monoclonal anti-PKA catalytic subunit, 10 μg/ml, BD #610980, and mouse monoclonal anti-PKA RIIβ, 10 μg/ml, BD #610625) diluted in blocking buffer for 2 hr and then secondary antibodies (Alexa-488- and 594-conjugated goat anti-mouse and rabbit antibodies respectively, Molecular Probes) for 1 hr at room temperature. Coverslips were mounted in Permafluor (Thermo Electron) and imaged using a confocal microscope (Zeiss, 63×, 1.4 NA).

Supplementary Material

Refer to Web version on PubMed Central for supplementary material.

Acknowledgments

We thank Stan McKnight for providing cDNAs of PKA subunits, Gareth Thomas for providing EGFP lentivirus particles, Graham Knott for providing electron microscopy data, Christopher Harvey and Ryohei Yasuda for discussions, Tim O'Connor for programming assistance, Barry Burbach, Xiaoqun Zhang, Nima Ghitani and Brenda Shields for experimental support, Karen Zito and Roberto Malinow for comments on the manuscript. This work was supported by HHMI, NIH, and the Essel Investigator Award of NARSAD (HZ).

References

Abel T, Nguyen PV, Barad M, Deuel TA, Kandel ER, Bourtchouladze R. Genetic demonstration of a role for PKA in the late phase of LTP and in hippocampus-based long-term memory. Cell 1997;88:615–626. [PubMed: 9054501]

Bauman AL, Goehring AS, Scott JD. Orchestration of synaptic plasticity through AKAP signaling complexes. Neuropharmacology 2004;46:299–310. [PubMed: 14975685]

Blitzer RD, Connor JH, Brown GP, Wong T, Shenolikar S, Iyengar R, Landau EM. Gating of CaMKII by cAMP-regulated protein phosphatase activity during LTP. Science 1998;280:1940–1942. [PubMed: 9632393]

Bloodgood BL, Sabatini BL. Neuronal activity regulates diffusion across the neck of dendritic spines. Science 2005;310:866–869. [PubMed: 16272125]

Brandon EP, Idzerda RL, McKnight GS. PKA isoforms, neural pathways, and behaviour: making the connection. Curr Opin Neurobiol 1997;7:397–403. [PubMed: 9232801]

Brandon EP, Logue SF, Adams MR, Qi M, Sullivan SP, Matsumoto AM, Dorsa DM, Wehner JM, McKnight GS, Idzerda RL. Defective motor behavior and neural gene expression in RIIbeta-protein kinase A mutant mice. J Neurosci 1998;18:3639–3649. [PubMed: 9570795]

Buxton IL, Brunton LL. Compartments of cyclic AMP and protein kinase in mammalian cardiomyocytes. J Biol Chem 1983;258:10233–10239. [PubMed: 6309796]

Byrne JH, Kandel ER. Presynaptic facilitation revisited: state and time dependence. J Neurosci 1996;16:425–435. [PubMed: 8551327]

Carr DW, Stofko-Hahn RE, Fraser ID, Cone RD, Scott JD. Localization of the cAMP-dependent protein kinase to the postsynaptic densities by A-kinase anchoring proteins. Characterization of AKAP 79. J Biol Chem 1992;267:16816–16823. [PubMed: 1512224]

Carter AG, Sabatini BL. State-dependent calcium signaling in dendritic spines of striatal medium spiny neurons. Neuron 2004;44:483–493. [PubMed: 15504328]

Chetkovich DM, Chen L, Stocker TJ, Nicoll RA, Bredt DS. Phosphorylation of the postsynaptic density-95 (PSD-95)/discs large/zona occludens-1 binding site of stargazin regulates binding to PSD-95 and synaptic targeting of AMPA receptors. J Neurosci 2002;22:5791–5796. [PubMed: 12122038]

Chevaleyre V, Heifets BD, Kaeser PS, Sudhof TC, Castillo PE. Endocannabinoid-mediated long-term plasticity requires cAMP/PKA signaling and RIM1alpha. Neuron 2007;54:801–812. [PubMed: 17553427]

Choi J, Ko J, Park E, Lee JR, Yoon J, Lim S, Kim E. Phosphorylation of stargazin by protein kinase A regulates its interaction with PSD-95. J Biol Chem 2002;277:12359–12363. [PubMed: 11805122]

De Camilli P, Moretti M, Donini SD, Walter U, Lohmann SM. Heterogeneous distribution of the cAMP receptor protein RII in the nervous system: evidence for its intracellular accumulation on microtubules, microtubule-organizing centers, and in the area of the Golgi complex. J Cell Biol 1986;103:189–203. [PubMed: 3522603]

Dehmelt L, Halpain S. The MAP2/Tau family of microtubule-associated proteins. Genome Biol 2005;6:204. [PubMed: 15642108]

Dubnau J, Chiang AS, Tully T. Neural substrates of memory: from synapse to system. J Neurobiol 2003;54:238–253. [PubMed: 12486707]

Ehlers MD. Reinsertion or degradation of AMPA receptors determined by activity-dependent endocytic sorting. Neuron 2000;28:511–525. [PubMed: 11144360]

Esteban JA, Shi SH, Wilson C, Nuriya M, Huganir RL, Malinow R. PKA phosphorylation of AMPA receptor subunits controls synaptic trafficking underlying plasticity. Nat Neurosci 2003;6:136–143. [PubMed: 12536214]

Francis SH, Corbin JD. Structure and function of cyclic nucleotide-dependent protein kinases. Annu Rev Physiol 1994;56:237–272. [PubMed: 8010741]

Frey U, Huang YY, Kandel ER. Effects of cAMP simulate a late stage of LTP in hippocampal CA1 neurons. Science 1993;260:1661–1664. [PubMed: 8389057]

Gelinas JN, Nguyen PV. Beta-adrenergic receptor activation facilitates induction of a protein synthesis-dependent late phase of long-term potentiation. J Neurosci 2005;25:3294–3303. [PubMed: 15800184]

Gelinas JN, Tenorio G, Lemon N, Abel T, Nguyen PV. Beta-adrenergic receptor activation during distinct patterns of stimulation critically modulates the PKA-dependence of LTP in the mouse hippocampus. Learn Mem 2008;15:281–289. [PubMed: 18441285]

Gleason MR, Higashijima S, Dallman J, Liu K, Mandel G, Fetcho JR. Translocation of CaM kinase II to synaptic sites in vivo. Nat Neurosci 2003;6:217–218. [PubMed: 12563265]

Goldsmith BA, Abrams TW. cAMP modulates multiple K+ currents, increasing spike duration and excitability in Aplysia sensory neurons. Proc Natl Acad Sci U S A 1992;89:11481–11485. [PubMed: 1333612]

Gomez LL, Alam S, Smith KE, Horne E, Dell'Acqua ML. Regulation of A-kinase anchoring protein 79/150-cAMP-dependent protein kinase postsynaptic targeting by NMDA receptor activation of calcineurin and remodeling of dendritic actin. J Neurosci 2002;22:7027–7044. [PubMed: 12177200]

Gray NW, Weimer RM, Bureau I, Svoboda K. Rapid Redistribution of Synaptic PSD-95 in the Neocortex In Vivo. PLoS Biol 2006:4.

Greenberg SM, Castellucci VF, Bayley H, Schwartz JH. A molecular mechanism for long-term sensitization in Aplysia. Nature 1987;329:62–65. [PubMed: 3041225]

Harada A, Teng J, Takei Y, Oguchi K, Hirokawa N. MAP2 is required for dendrite elongation, PKA anchoring in dendrites, and proper PKA signal transduction. J Cell Biol 2002;158:541–549. [PubMed: 12163474]

Harvey CD, Svoboda K. Locally dynamic synaptic learning rules in pyramidal neuron dendrites. Nature 2007;450:1195–1200. [PubMed: 18097401]

Hausken ZE, Coghlan VM, Hastings CA, Reimann EM, Scott JD. Type II regulatory subunit (RII) of the cAMP-dependent protein kinase interaction with A-kinase anchor proteins requires isoleucines 3 and 5. J Biol Chem 1994;269:24245–24251. [PubMed: 7929081]

Herberg FW, Maleszka A, Eide T, Vossebein L, Tasken K. Analysis of A-kinase anchoring protein (AKAP) interaction with protein kinase A (PKA) regulatory subunits: PKA isoform specificity in AKAP binding. J Mol Biol 2000;298:329–339. [PubMed: 10764601]

Hoffman DA, Johnston D. Downregulation of transient K^+ chanels in dendrites of hippocampal CA1 pyramidal neurons by activation of PKA and PKC. J Neurosci 1998;18:3521–3528. [PubMed: 9570783]

Hoshi N, Langeberg LK, Scott JD. Distinct enzyme combinations in AKAP signalling complexes permit functional diversity. Nat Cell Biol 2005;7:1066–1073. [PubMed: 16228013]

Hu H, Real E, Takamiya K, Kang MG, Ledoux J, Huganir RL, Malinow R. Emotion enhances learning via norepinephrine regulation of AMPA-receptor trafficking. Cell 2007;131:160–173. [PubMed: 17923095]

Husi H, Ward MA, Choudhary JS, Blackstock WP, Grant SG. Proteomic analysis of NMDA receptor-adhesion protein signaling complexes. Nat Neurosci 2000;3:661–669. [PubMed: 10862698]

Impey S, Goodman RH. CREB signaling--timing is everything. Sci STKE 2001 2001:PE1.

Inan M, Lu HC, Albright MJ, She WC, Crair MC. Barrel map development relies on protein kinase A regulatory subunit II beta-mediated cAMP signaling. J Neurosci 2006;26:4338–4349. [PubMed: 16624954]

Iyengar R. Gating by cyclic AMP: expanded role for an old signaling pathway. Science 1996;271:461–463. [PubMed: 8560257]

Khuchua Z, Wozniak DF, Bardgett ME, Yue Z, McDonald M, Boero J, Hartman RE, Sims H, Strauss AW. Deletion of the N-terminus of murine map2 by gene targeting disrupts hippocampal ca1 neuron architecture and alters contextual memory. Neuroscience 2003;119:101–111. [PubMed: 12763072]

Lee HK, Barbarosie M, Kameyama K, Bear MF, Huganir RL. Regulation of distinct AMPA receptor phosphorylation sites during bidirectional synaptic plasticity. Nature 2000;405:955–959. [PubMed: 10879537]

Leenders AG, Sheng ZH. Modulation of neurotransmitter release by the second messenger-activated protein kinases: implications for presynaptic plasticity. Pharmacol Ther 2005;105:69–84. [PubMed: 15626456]

Lin JW, Wyszynski M, Madhavan R, Sealock R, Kim JU, Sheng M. Yotiao, a novel protein of neuromuscular junction and brain that interacts with specific splice variants of NMDA receptor subunit NR1. J Neurosci 1998;18:2017–2027. [PubMed: 9482789]

Lin MT, Lujan R, Watanabe M, Adelman JP, Maylie J. SK2 channel plasticity contributes to LTP at Schaffer collateral-CA1 synapses. Nat Neurosci 2008;11:170–177. [PubMed: 18204442]

Lu Y, Allen M, Halt AR, Weisenhaus M, Dallapiazza RF, Hall DD, Usachev YM, McKnight GS, Hell JW. Age-dependent requirement of AKAP150-anchored PKA and GluR2-lacking AMPA receptors in LTP. Embo J 2007;26:4879–4890. [PubMed: 17972919]

Lu Y, Zhang M, Lim IA, Hall DD, Allen M, Medvedeva Y, McKnight GS, Usachev YM, Hell JW. AKAP150-anchored PKA activity is important for LTD during its induction phase. J Physiol 2008;586:4155–4164. [PubMed: 18617570]

Man HY, Sekine-Aizawa Y, Huganir RL. Regulation of {alpha}-amino-3-hydroxy-5-methyl-4-isoxazolepropionic acid receptor trafficking through PKA phosphorylation of the Glu receptor 1 subunit. Proc Natl Acad Sci U S A 2007;104:3579–3584. [PubMed: 17360685]

Matsuzaki M, Ellis-Davies GC, Nemoto T, Miyashita Y, Iino M, Kasai H. Dendritic spine geometry is critical for AMPA receptor expression in hippocampal CA1 pyramidal neurons. Nat Neurosci 2001;4:1086–1092. [PubMed: 11687814]

Meyer T, Shen K. In and out of the postsynaptic region: signalling proteins on the move. Trends Cell Biol 2000;10:238–244. [PubMed: 10802539]

Montminy M. Transcriptional activation. Something new to hang your HAT on. Nature 1997;387:654–655. [PubMed: 9192883]

Myme CI, Sugino K, Turrigiano GG, Nelson SB. The NMDA-to-AMPA ratio at synapses onto layer 2/3 pyramidal neurons is conserved across prefrontal and visual cortices. J Neurophysiol 2003;90:771–779. [PubMed: 12672778]

Oh MC, Derkach VA, Guire ES, Soderling TR. Extrasynaptic membrane trafficking regulated by GluR1 serine 845 phosphorylation primes AMPA receptors for long-term potentiation. J Biol Chem 2006;281:752–758. [PubMed: 16272153]

Otmakhova NA, Lisman JE. D1/D5 dopamine receptors inhibit depotentiation at CA1 synapses via cAMP-dependent mechanism. J Neurosci 1998;18:1270–1279. [PubMed: 9454837]

Patterson GH, Lippincott-Schwartz J. A photoactivatable GFP for selective photolabeling of proteins and cells. Science 2002;297:1873–1877. [PubMed: 12228718]

Pedarzani P, Storm JF. PKA mediates the effects of monoamine transmitters on the K+ current underlying the slow spike frequency adaptation in hippocampal neurons. Neuron 1993;11:1023–1035. [PubMed: 8274274]

Pologruto TA, Sabatini BL, Svoboda K. ScanImage: Flexible software for operating laser-scanning microscopes. BioMedical Engineering OnLine 2003;2:13. [PubMed: 12801419]

Raman IM, Tong G, Jahr CE. Beta-adrenergic regulation of synaptic NMDA receptors by cAMP-dependent protein kinase. Neuron 1996;16:415–421. [PubMed: 8789956]

Rich TC, Fagan KA, Tse TE, Schaack J, Cooper DM, Karpen JW. A uniform extracellular stimulus triggers distinct cAMP signals in different compartments of a simple cell. Proc Natl Acad Sci U S A 2001;98:13049–13054. [PubMed: 11606735]

Rosenmund C, Carr DW, Bergeson SE, Nilaver G, Scott JD, Westbrook GL. Anchoring of protein kinase A is required for modulation of AMPA/kainate receptors on hippocampal neurons. Nature 1994;368:853–856. [PubMed: 8159245]

Saito T, Nakatsuji N. Efficient gene transfer into the embryonic mouse brain using in vivo electroporation. Dev Biol 2001;240:237–246. [PubMed: 11784059]

Scott JD. Cyclic nucleotide-dependent protein kinases. Pharmacol Ther 1991;50:123–145. [PubMed: 1653962]

Shaner NC, Campbell RE, Steinbach PA, Giepmans BN, Palmer AE, Tsien RY. Improved monomeric red, orange and yellow fluorescent proteins derived from Discosoma sp. red fluorescent protein. Nat Biotechnol. 2004

Shaywitz AJ, Greenberg ME. CREB: a stimulus-induced transcription factor activated by a diverse array of extracellular signals. Annu Rev Biochem 1999;68:821–861. [PubMed: 10872467]

Shen K, Meyer T. Dynamic control of CaMKII translocation and localization in hippocampal neurons by NMDA receptor stimulation. Science 1999;284:162–166. [PubMed: 10102820]

Snyder EM, Colledge M, Crozier RA, Chen WS, Scott JD, Bear MF. Role for A kinase-anchoring proteins (AKAPS) in glutamate receptor trafficking and long term synaptic depression. J Biol Chem 2005;280:16962–16968. [PubMed: 15718245]

Sobczyk A, Scheuss V, Svoboda K. NMDA receptor subunit-dependent [Ca2+] signaling in individual hippocampal dendritic spines. J Neurosci 2005;25:6037–6046. [PubMed: 15987933]

Stoppini L, Buchs PA, Muller DA. A simple method for organotypic cultures of nervous tissue. J Neurosci Methods 1991;37:173–182. [PubMed: 1715499]

Sun X, Zhao Y, Wolf ME. Dopamine receptor stimulation modulates AMPA receptor synaptic insertion in prefrontal cortex neurons. J Neurosci 2005;25:7342–7351. [PubMed: 16093384]

Swayze RD, Lise MF, Levinson JN, Phillips A, El-Husseini A. Modulation of dopamine mediated phosphorylation of AMPA receptors by PSD-95 and AKAP79/150. Neuropharmacology 2004;47:764–778. [PubMed: 15458848]

Tabata H, Nakajima K. Efficient in utero gene transfer system to the developing mouse brain using electroporation: visualization of neuronal migration in the developing cortex. Neuroscience 2001;103:865–872. [PubMed: 11301197]

Tasken K, Aandahl EM. Localized effects of cAMP mediated by distinct routes of protein kinase A. Physiol Rev 2004;84:137–167. [PubMed: 14715913]

Tavalin SJ, Colledge M, Hell JW, Langeberg LK, Huganir RL, Scott JD. Regulation of GluR1 by the A-kinase anchoring protein 79 (AKAP79) signaling complex shares properties with long-term depression. J Neurosci 2002;22:3044–3051. [PubMed: 11943807]

Theurkauf WE, Vallee RB. Molecular characterization of the cAMP-dependent protein kinase bound to microtubule-associated protein 2. J Biol Chem 1982;257:3284–3290. [PubMed: 6277931]

Thomas MJ, Moody TD, Makhinson M, O'Dell TJ. Activity-dependent beta-adrenergic modulation of low frequency stimulation induced LTP in the hippocampal CA1 region. Neuron 1996;17:475–482. [PubMed: 8816710]

Tunquist BJ, Hoshi N, Guire ES, Zhang F, Mullendorff K, Langeberg LK, Raber J, Scott JD. Loss of AKAP150 perturbs distinct neuronal processes in mice. Proc Natl Acad Sci U S A 2008;105:12557–12562. [PubMed: 18711127]

Turner KM, Burgoyne RD, Morgan A. Protein phosphorylation and the regulation of synaptic membrane traffic. Trends Neurosci 1999;22:459–464. [PubMed: 10481193]

Tzounopoulos T, Janz R, Sudhof TC, Nicoll RA, Malenka RC. A role for cAMP in long-term depression at hippocampal mossy fiber synapses. Neuron 1998;21:837–845. [PubMed: 9808469]

Ventra C, Porcellini A, Feliciello A, Gallo A, Paolillo M, Mele E, Avvedimento VE, Schettini G. The differential response of protein kinase A to cyclic AMP in discrete brain areas correlates with the abundance of regulatory subunit II. J Neurochem 1996;66:1752–1761. [PubMed: 8627334]

Weisskopf MG, Castillo PE, Zalutsky RA, Nicoll RA. Mediation of hippocampal mossy fiber long-term potentiation by cyclic AMP. Science 1994;265:1878–1882. [PubMed: 7916482]

Westphal RS, Tavalin SJ, Lin JW, Alto NM, Fraser ID, Langeberg LK, Sheng M, Scott JD. Regulation of NMDA receptors by an associated phosphatase-kinase signaling complex. Science 1999;285:93–96. [PubMed: 10390370]

Winder DG, Martin KC, Muzzio IA, Rohrer D, Chruscinski A, Kobilka B, Kandel ER. ERK plays a regulatory role in induction of LTP by theta frequency stimulation and its modulation by beta-adrenergic receptors. Neuron 1999;24:715–726. [PubMed: 10595521]

Wong W, Scott JD. AKAP signalling complexes: focal points in space and time. Nat Rev Mol Cell Biol 2004;5:959–970. [PubMed: 15573134]

Yasuda H, Barth AL, Stellwagen D, Malenka RC. A developmental switch in the signaling cascades for LTP induction. Nat Neurosci 2003;6:15–16. [PubMed: 12469130]

Zaccolo M, Pozzan T. Discrete microdomains with high concentration of cAMP in stimulated rat neonatal cardiac myocytes. Science 2002;295:1711–1715. [PubMed: 11872839]

Zacharias DA, Violin JD, Newton AC, Tsien RY. Partitioning of lipid-modified monomeric GFPs into membrane microdomains of live cells. Science 2002;296:913–916. [PubMed: 11988576]

Zito K, Scheuss V, Knott G, Hill T, Svoboda K. Rapid functional maturation of nascent dendritic spines. Neuron 2009;61:247–258. [PubMed: 19186167]

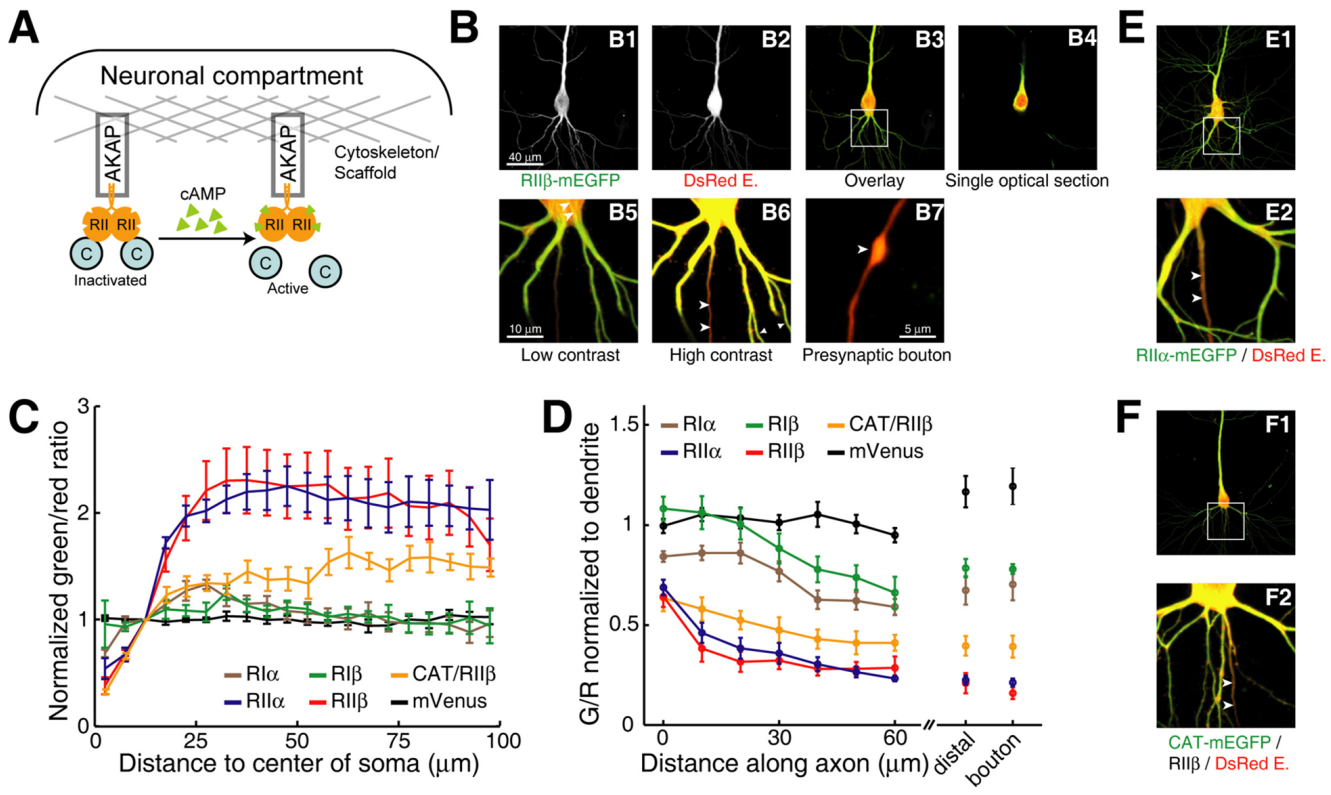

Figure 1. Type II PKA is enriched in the dendrite and excluded from the axon

(A) Schematic targeting and activation of type II PKA.

(B) Representative two-photon images of a CA1 neuron in a cultured hippocampal slice that was co-transfected with RIIβ-mEGFP and DsRed Express. All but B4 are maximum value projections. White box in B3 correspond to the blow-ups in B5 and B6. Arrowheads: B5, a cytoskeletal structure; in B6, axon; B7, presynaptic bouton. Triangles in B6 point to thin dendrites without saturated pixels. Pixel sizes: B1-4, 0.31 μm; B5–7, 0.08 μm.

(C) Green/red ratios along the radius away from the center of the soma (see **Experimental Procedures** for definition). For the CAT/RIIβ combination (orange), CAT was tagged with mEGFP and RIIβ was untagged. All data were normalized to the value at 12.5 μm from the center of the soma before averaging. n = 5 for mVenus, RIβ and CAT/RIIβ; n = 6 for RIα, RIIα and RIIβ.

(D) Green/red ratios along proximal axons, in distal axons, and in boutons. Values are normalized to the G/R of thin basal dendrites.

(E) Representative image of CA1 neuron expressing RIIα-mEGFP and DsRed Express.

(F) Representative image of CA1 neurons expressing CAT-mEGFP, RIIβ and DsRed Express. Scales of panels E and F are the same as B1 and B5.

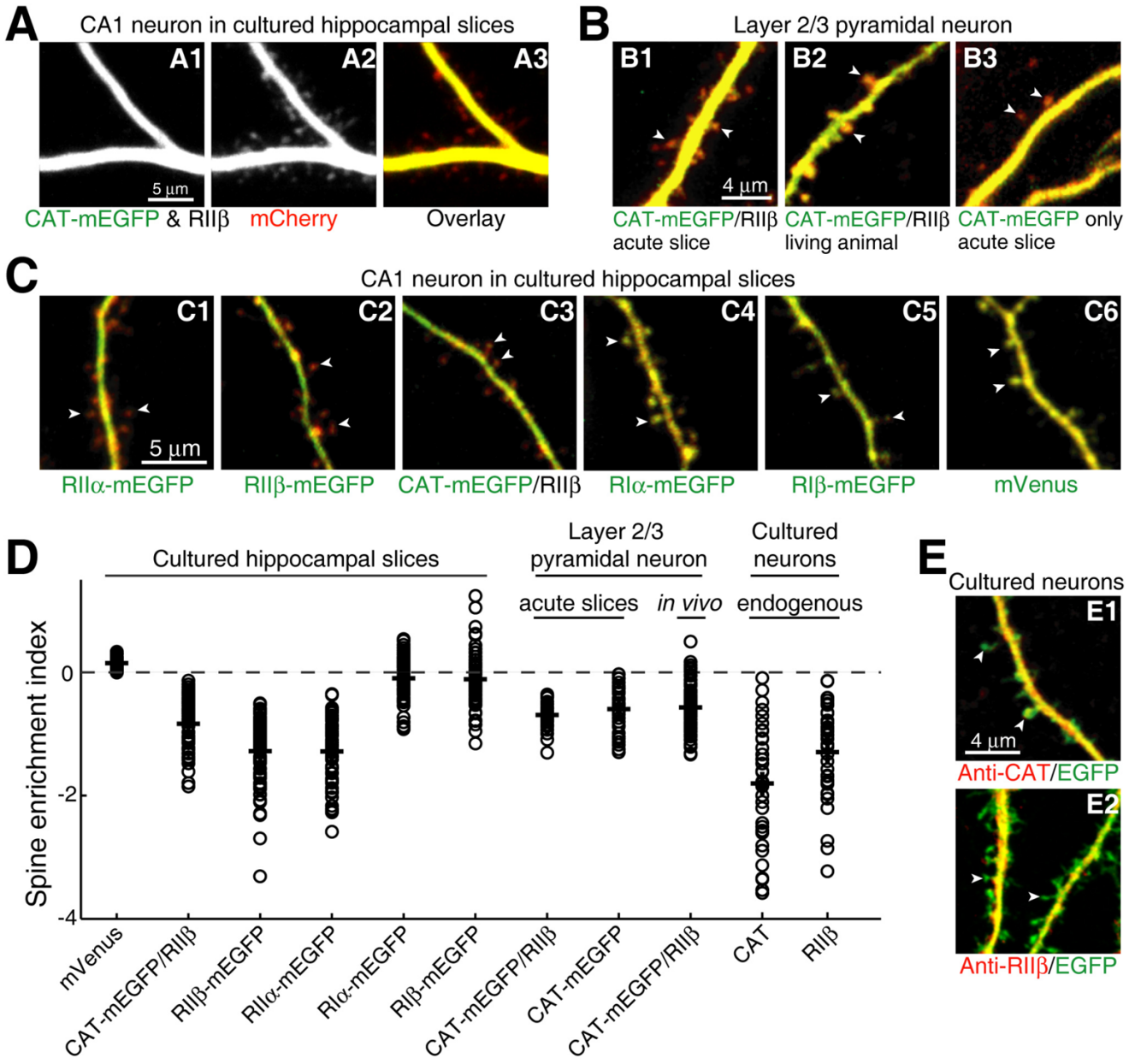

Figure 2. Type II PKA was excluded from spine in hippocampal CA1 neurons and layer 2/3 cortical pyramidal neurons *in vitro* and *in vivo*

(A) Representative images (256×256 pixels, 0.07 μm per pixel) showing spines and their parental dendrites of a CA1 neuron in cultured hippocampal slices that was transfected with CAT-mEGFP, RIIβ and mCherry. Images from individual color channels are shown in grayscale.

(B) Representative images (0.10 μm per pixel). Layer 2/3 pyramidal neurons in the somatosensory cortex were transfected by *in utero* electroporation with CAT-mEGFP and DsRed Express. With (B1, B2) or without (B3) exogenous RIIβ. Arrowheads indicate representative spines.

(C) Representative images (0.08 μm per pixel). CA1 pyramidal neurons in cultured hippocampal slices were transfected with DsRed Express and the indicated constructs.

(D) Spine enrichment index (SEI) measurements of experiments shown in B, C and E.
(E) Representative images (0.07 μm per pixel) indicating that endogenous PKA is enriched in dendritic shafts. Note that the colors for the protein of interest and the cytosol marker are reversed compared to the other experiments. Immunostaining (red) was for PKA catalytic subunits (CAT) or RIIβ on dissociated hippocampal neuronal cultures expressing EGFP (green).

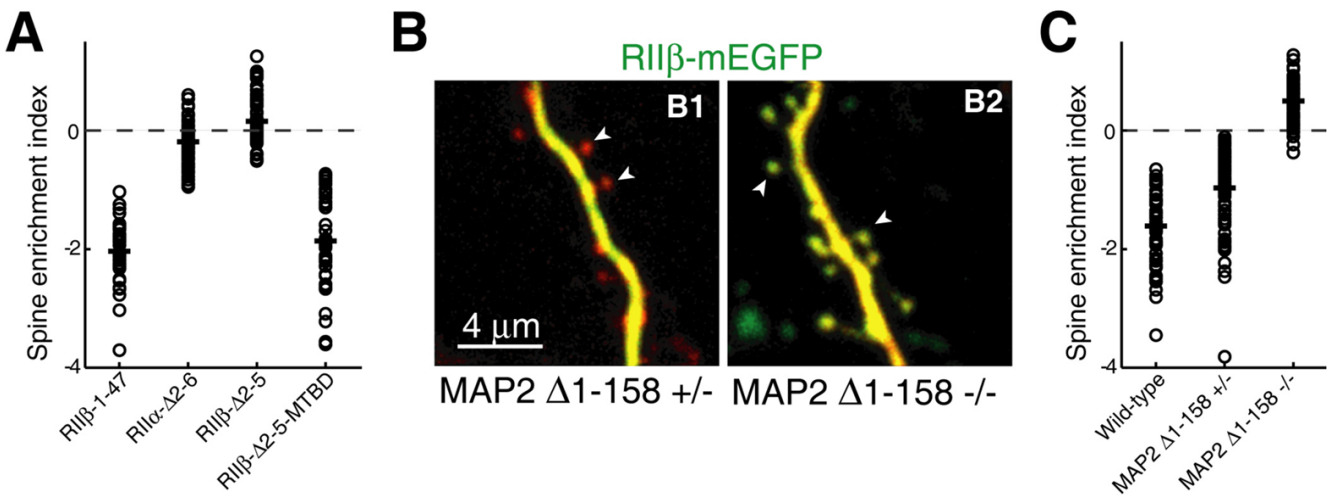

Figure 3. Dendritic targeting of type II PKA is mediated by MAP2

(A) Structure-function studies on type II regulatory subunits. All constructs were tagged with mEGFP. For RIIβ-Δ 2–5-MTBD, the microtubule-binding domain (P272-end) of human MAP2c was tagged on the C-terminus of RIIβ-Δ 2–5.

(B, C) Representative images (0.10 μm per pixel) and SEI measurements of CA1 neurons in cultured hippocampal slices prepared from MAP2Δ1–158 −/− mice, their heterozygous littermates and wild-type. RIIβ-mEGFP and DsRed Express were expressed.

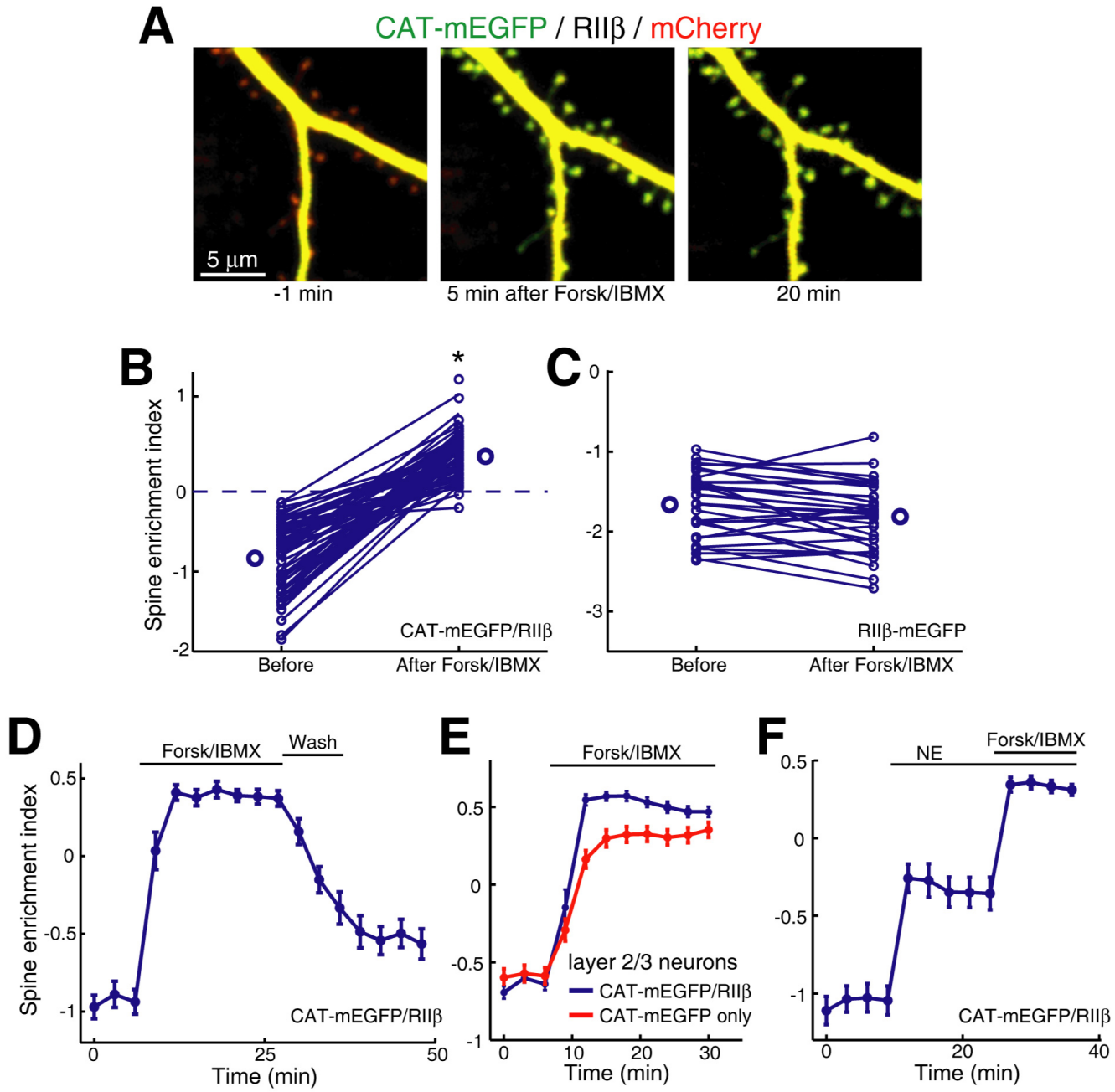

Figure 4. PKA catalytic subunit redistributes to become enriched in spines upon activation

(A, B) Representative spine-dendrite images (0.07 μm per pixel) and collective SEI measurements of CA1 neurons expressing CAT-mEGFP, RIIβ and mCherry, before and after bath application of 50μM forskolin and 100 μM IBMX. *, significantly bigger than 0.

(C) RIIβ-mEGFP did not move upon forskolin and IBMX activation.

(D) Time course and reversibility of the catalytic subunit moving into spines. n = 34.

(E) Catalytic subunits expressed in layer 2/3 pyramidal neurons of somatosensory cortex from mice *in utero* electroporated with CAT-mEGFP and DsRed Express also moved to become enriched in spines. With (blue, n = 31) or without (red, n = 41) exogenous RIIβ.

(F) Norepinephrine (NE) could initiate the movement of the catalytic subunit into spines. n = 40.

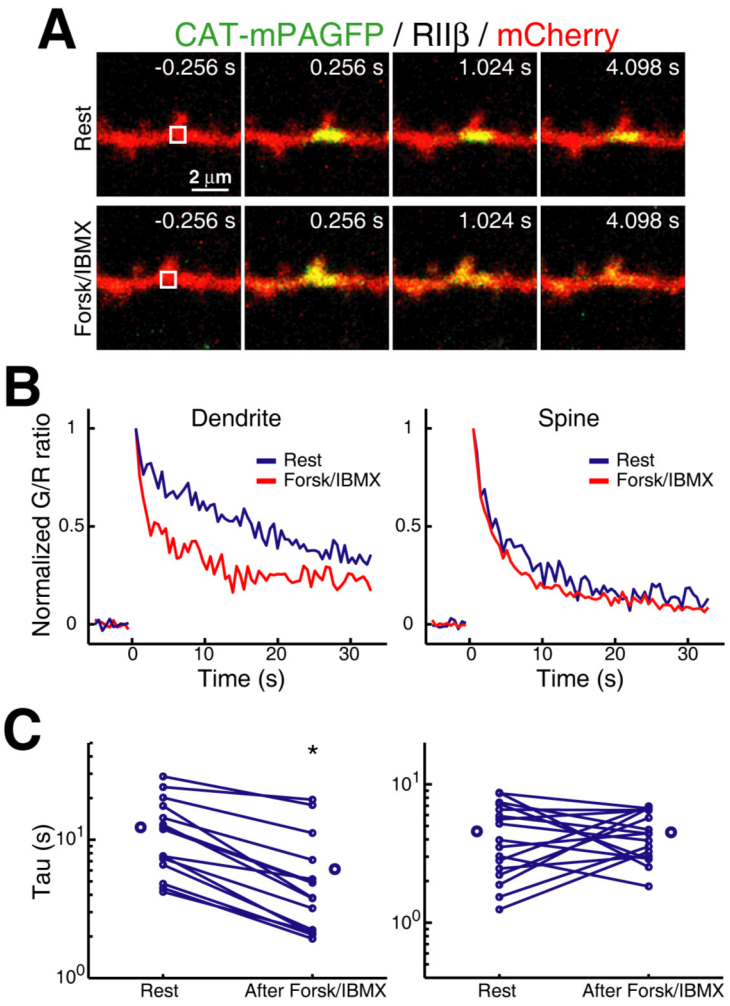

Figure 5. PKA catalytic subunit diffused faster in dendrites upon forskolin and IBMX activation

(A) Representative time-lapse images (0.06 μm per pixel). CA1 neurons were expressing CAT-PAGFP, RIIβ and mCherry. Photoactivation was achieved by a nearly instantaneous pulse (~20 ms) of 810nm illumination within the white boxes at 0s.

(B) Representative traces of the remaining fluorescence within the activated area. Activation was at the dendrite (left, same as images in panel A) or at the spine (right, the spine above the white box in panel A).

(C) Collective decay time constants for dendrites (left) and spines (right). *, significantly smaller.

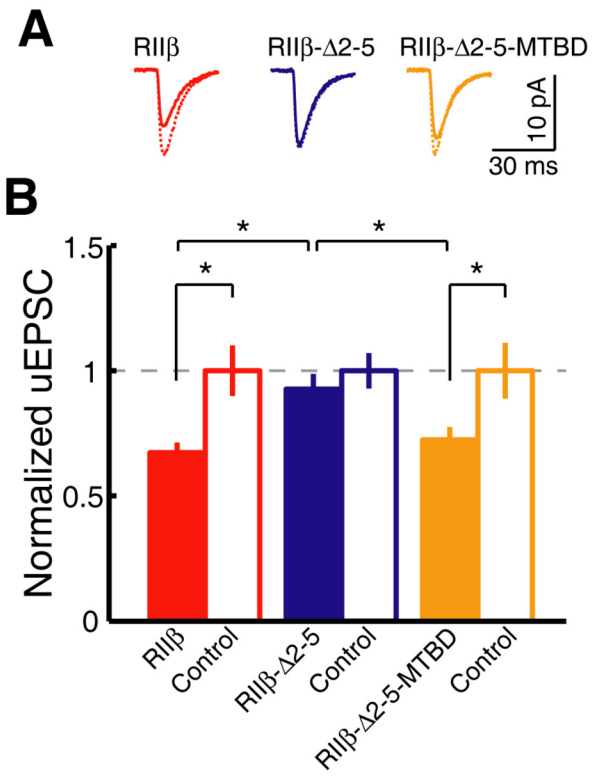

Figure 6. Dendritic enrichment of type II PKA is important for regulating AMPA receptor contents in spines

(A) Averaged uEPSC of all response traces from layer 2/3 pyramidal neurons expressing indicated mEGFP-tagged constructs (solid lines) and untransfected controls from the same slices (dash lines).

(B) Averaged peak amplitudes normalized to the same-slice control. *, significantly different. The volumes between the transfected spines and untransfected controls were not significantly different for all pairs.

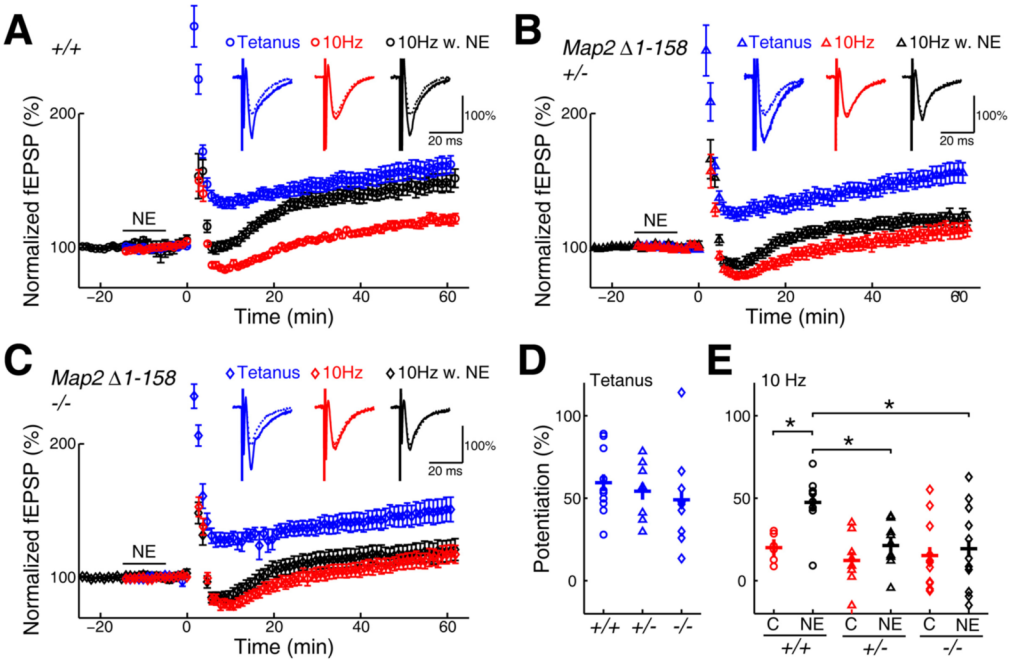

Figure 7. The binding between MAP2 and type II PKA is necessary for norepinephrine facilitation of LTP induction

(A, B and C) Representative traces and averaged, normalized field EPSP amplitudes measured from wild-type, heterozygous and homozygous littermates of *MAP2Δ1–158 mice*. LTP were induced with 2 trains of 1s 100 Hz stimulation (blue) or with 900 pulses of 10 Hz stimulation (red and black). For black traces, norepinephrine was applied at -15 to -5 minutes.

(D, E) Average potentiation from 50 to 60 minutes by the tetanus LTP induction protocol or the 10 Hz protocol. *, significantly different.